Progress In Electromagnetics Research M, Vol. 92, 67–78, 2020

Research on Channel Model of Broadband Power Line Communication Based on MTL and Radiation Effect

Xueyu Duan[1], Yizhen Wei[1], Donglin He[1, 2], Zili Xu[2], Hong Zhang[1] and Wei Hua[1, *]

Abstract—Nowadays, the key to design a reliable communication system is to acquire channel characteristics and improve channel capacity. In the transmission of high-speed data, the unshielded transmission channel used in power line communication has interference factors such as noise, attenuation, reflection, radiation, and time-varying. A three-wire MIMO-PLC channel transfer function priori model has been established based on the theory of MTL in this paper, which is necessary for band pre-selection, power setting, and dynamic range design in a high-speed MIMO-PLC set to improve the unshielded transmission channel capacity with the effect of noise, attenuation, reaction, radiation, and time-varying factors. The simulation results with the model parameters of geometric sizes, material, surrounding medium, and lengths of the power line network agree well with the measurement ones in the frequency band of 1–200 MHz. The research results of this paper have guiding significance for the band pre-selection, power setting, and dynamic range design of broadband MIMO-PLC.

1. INTRODUCTION

Power line communication (PLC) has been developed rapidly in the fields of internet high-speed access, video monitoring, smart home, mine safety management, electric vehicle management, etc. [1, 2], and also applied to airport control system [3]. In particular, the cost will be high if cables are laid again in areas where control cables or communication cables were not laid during airport construction. Therefore, the widespread existence of power line network makes PLC technology become a potential important means in the field of airport communication and monitoring. Compared with the traditional single input single output PLC (SISO-PLC), multiple input multiple output PLC (MIMO-PLC) [4, 5] can use multiple channels to improve communication quality, enhance reliability, increase transmission range, and improve throughput [6, 7], which is considered as a potential and effective means of PLC development in the future, and is widely accepted by the industry. However, it is necessary to analyze PLC channel to improve its transmission performance and reliability because of the influence of radiation, noise, fading, and multipath on PLC channel characteristics [8, 9]. Therefore, modeling and analyzing the coupling between electromagnetic wave and power line is an important research content in the field of electromagnetic compatibility [10]. At present, there are many research results related to the accurate channel transmission characteristics of various power line networks. The bottom-up modeling method is used in [11] to calculate the channel transfer function by applying the voltage ratio method. A random PLC channel generator with a frequency range of 1–100 MHz has been given in [12]. All of the above models are based on the channel transfer function obtained from the power line measurement data in different environments, which fails to realize the prior research on the power line channel characteristics. In [13], according to MTL theory, a common mode current propagation model of a three-wire power line network in the frequency range of 1–30 MHz has been proposed. In [14], the influence of conduction and radiation on signal integrity is analyzed, and the unit length equivalent

Received 10 January 2020, Accepted 26 April 2020, Scheduled 6 May 2020
* Corresponding author: Wei Hua (huaw@scu.edu.cn).
[1] College of Electronics and Information Engineering at Sichuan University, Chengdu 610065, China. [2] The Second Research Institute of Civil Aviation Administration of China, Chengdu 610041, China.

circuit including radiation resistance has been given. References [13, 14] give some analysis on the impedance or radiation of the power line, but the transfer function model with radiation loss is not established. In [18], a two-wire model with radiation loss is proposed.

In order to accurately estimate the channel attenuation and spectrum characteristics of complex power line network and provide guidance for band pre-selection, power setting, and dynamic range design of broadband MIMO-PLC, the channel model needs to be improved. Therefore, this paper proposes a three-wire transfer function model with radiation loss based on the existing MIMO-PLC channel model, which is suitable for 1–200 MHz frequency band and also suitable for 1–100 MHz mainstream frequency band.

This paper is organized as follows. Section 2 illustrates some foundation concepts to build the power line BPLC model, including revision of radiation resistance by common mode and differential mode radiation loss of long wire antenna. Section 3 adds the radiation loss to the three-wire power line channel modeling. In Section 4, the accuracy of the proposed irradiate model is elucidated by comparing the simulated results with the measured ones. Finally, the contribution of the research is given in Section 5.

2. BASIC PARAMETERS OF THREE-WIRE POWER LINE CHANNEL MODELING

2.1. Equivalent Distribution Parameters

A three-wire power line is equivalent to a three-conductor transmission line in this paper. The distributed parameters per unit length can be stated as Inductance L, Capacitance C, Resistance R, and Conductivity G

$$\begin{aligned} L &= \begin{bmatrix} l_1 & l_m \\ l_m & l_2 \end{bmatrix} \\ C &= \begin{bmatrix} c_1 + c_m & -c_m \\ -c_m & c_2 + c_m \end{bmatrix} \\ G &= \begin{bmatrix} g_1 + g_m & -g_m \\ -g_m & g_2 + g_m \end{bmatrix} \\ R &= \begin{bmatrix} r_1^{Ohm} + r_0^{Ohm} & r_0^{Ohm} \\ r_0^{Ohm} & r_2^{Ohm} + r_0^{Ohm} \end{bmatrix} \end{aligned} \tag{1}$$

where l_1 and l_2, c_1 and c_2, g_1 and g_2, r_0^{Ohm}, r_1^{Ohm} and r_2^{Ohm} and the inductance, capacitance, conductivity, and resistance representing the unit length distribution parameters of the three-conductor transmission line, respectively. The interaction between conductors is represented by inductance l_m, capacitance c_m, and conductance g_m. Fig. 1 shows the cross section of the three-conductor symmetrical structure power line and three-conductor ribbon structure power line commonly used in engineering wiring. Among them, r_w is the radius of the inner conductor, d the distance between power lines, ε the equivalent permittivity, μ the permeability, σ_1 the conductivity, and σ_2 the conductivity of the medium between conductors.

Elements in matrix L:

$$l_1 = l_2 = 2l_m = \frac{\mu}{\pi} \ln\left(\frac{d}{r_w}\right) \tag{2}$$

The parameter matrices L, C, and G of unit length have the following relations:

$$\begin{aligned} LC &= CL = \mu\varepsilon I_2 \\ LG &= GL = \mu\sigma_2 I_2 \end{aligned} \tag{3}$$

where I_2 is the unit matrix. The inductance matrix L, capacitance matrix C, and conductivity matrix G can be obtained from Eqs. (2) and (3). The elements of the resistance matrix R are calculated as follows:

$$r^{Ohm} = \begin{cases} \dfrac{1}{\sigma_1 \pi {r_w}^2}, & r_w < 2\delta \\ \dfrac{1}{2\pi r_w}\sqrt{\dfrac{\omega\mu}{2\sigma_1}}, & r_w > 2\delta \end{cases} \tag{4}$$

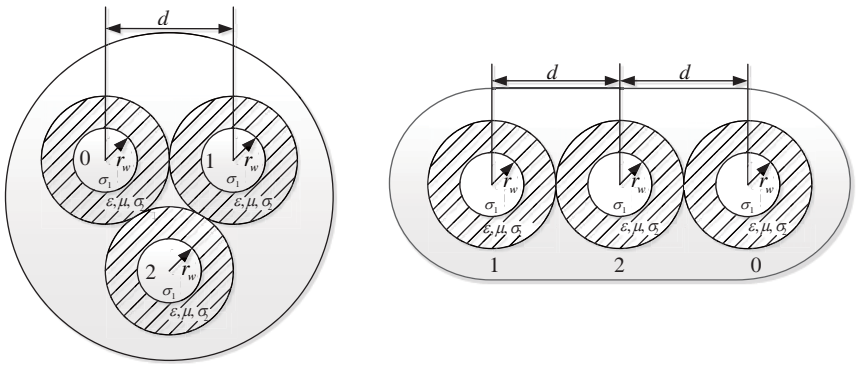

Figure 1. Symmetrical structure and ribbon structure.

where δ is the skin depth.

$$\delta = \sqrt{\frac{2}{\omega\mu\sigma_1}} = \frac{1}{\sqrt{\pi f\mu\sigma_1}} \tag{5}$$

If three conductors of the three-wire power line have the same geometric and electrical characteristics, then the elements in the resistance matrix R of unit length are obtained, which are $r_0^{Ohm} = r_1^{Ohm} = r_2^{Ohm}$. When $r_w < 2\delta$, the low frequency current can pass through the whole cross section; when $r_w > 2\delta$, it can be calculated by skin effect.

For a three-conductor transmission line, both phasor voltage $V(z)$ and phasor current $I(z)$ are 2×1 column vectors, and the complex matrices T_V and T_I are 2×2 nonsingular matrices, that is, T_V^{-1} and T_I^{-1} exist. The complex matrix T_V is defined as the variable transformation between the actual phasor voltage $V_{(z)}$ and mode voltage $V_m(z)$, and the complex matrix T_I is defined as the variable transformation between the actual phasor current $I(z)$ and mode current $I_m(z)$ on the transmission line.

In three-conductor symmetrical transmission lines, Z is the impedance matrix of unit length; Y is the admittance matrix of unit length; Z and Y matrices are reciprocal.

$$\begin{aligned} Z &= R + \mathrm{j}\omega L \\ Y &= G + \mathrm{j}\omega C \end{aligned} \tag{6}$$

The MTL equation of the second order is

$$\begin{aligned} \frac{\mathrm{d}^2}{\mathrm{d}z^2} V_{\mathrm{m}}(z) &= T_V^{-1} Z Y T_V V_{\mathrm{m}}(z) = \Lambda V_{\mathrm{m}}(z) \\ \frac{\mathrm{d}^2}{\mathrm{d}z^2} I_{\mathrm{m}}(z) &= T_I^{-1} Y Z T_I I_{\mathrm{m}}(z) = \Lambda I_{\mathrm{m}}(z) \end{aligned} \tag{7}$$

Here, Λ is a 2×2 eigenvalue diagonal matrix [15, 16]

$$\Lambda = \begin{bmatrix} {\gamma_1}^2 & 0 \\ 0 & {\gamma_2}^2 \end{bmatrix} \tag{8}$$

where γ_1 and γ_2 are propagation constants; α is the attenuation constant matrix; and β is the phase constant matrix. The propagation constant matrix γ is

$$\gamma = \sqrt{\Lambda} = \begin{bmatrix} \gamma_1 & 0 \\ 0 & \gamma_2 \end{bmatrix} = \alpha + \mathrm{j}\beta \tag{9}$$

As shown in Fig. 2, $N + 2$ nodes are divided into $N + 1$ main power lines with the shortest path between the sender and the receiver as the backbone, where l_x is the length of each main power line segment; the branch equivalent admittance matrix of each node is defined as Y_{bx}; Y_{inx} is the input admittance matrix of each node; and the equivalent admittance matrix of each node end is defined as Y_{eqx}.

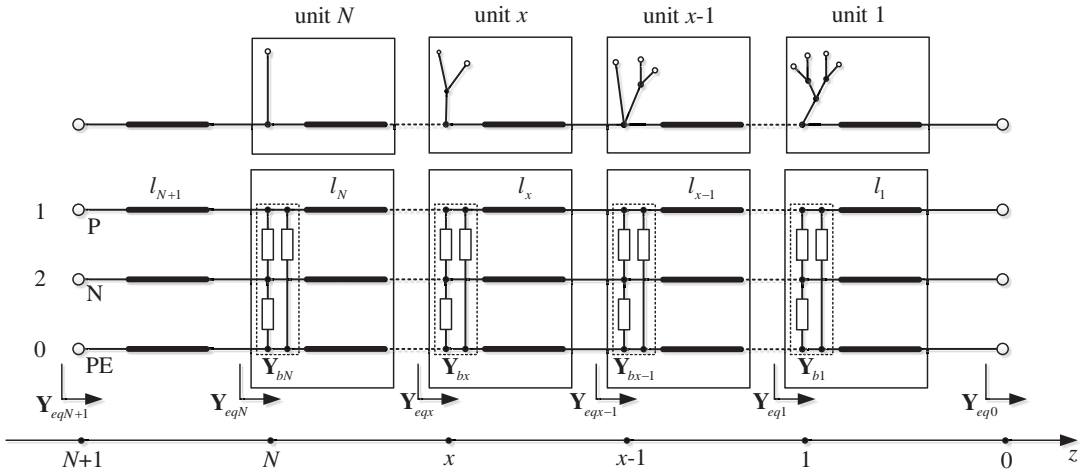

Figure 2. Power line network unit.

The equivalent admittance matrix of each node end is

$$Y_{eqx}(x) = Y_{inx}(x) + Y_{bx}(x) \tag{10}$$

Γ_V is the reflection coefficient matrix of voltage, and Y_0 is the characteristic admittance matrix.

$$Y_0 = Z^{-1} T_V \gamma T_V^{-1} \tag{11}$$

$$Y_{inx}(x) = Y_0 \left[I_2 - T_V e^{-\gamma x} \Gamma_V (x-1) T_V e^{-\gamma x} T_V^{-1} \right] \left[I_2 + T_V e^{-\gamma x} \Gamma_V (x-1) T_V e^{-\gamma x} T_V^{-1} \right]^{-1} \tag{12}$$

$$\Gamma_V (x-1) = \frac{Y_0 - Y_{eqx}(x-1)}{Y_0 + Y_{eqx}(x-1)} \tag{13}$$

Similarly, we can get Y_{bx}. Γ_I is the reflection coefficient matrix of current.

$$\Gamma_I(x) = \frac{Y_{eqx}(x) + Y_0}{Y_{eqx}(x) - Y_0} \tag{14}$$

The relationship between current reflection coefficient matrix and voltage reflection coefficient matrix is

$$\Gamma_I(x) = -Y_0 \Gamma_V(x) {Y_0}^{-1} \tag{15}$$

2.2. Revision of Radiation Resistance by Common Mode and Differential Mode Radiation Loss of Long Wire Antenna

In the actual transmission line, there is a case where the sum of current on any cross section is not zero, which is called "antenna current". Therefore, the total current flowing through the transmission line is divided into common mode current and differential mode current [17]. Considering that the power line network is in the mismatched state in general, we introduce the MIMP-PLC channel transfer function radiation model which adds the radiation loss factor in the mismatched state to simulate the transmission characteristics of the three-wire power line network channel.

Suppose that the parallel two-wire transmission line could be equivalent to a long wire antenna and its mirror image under the ground, as shown in Fig. 3(a). The radiation loss can be imported into the transfer function model of power line channel [18]. The antenna with a length of l is placed along the z-axis, with the feeding point placed at the origin of the coordinate. I^+ and I^- represent the incident wave current and reflected wave current in the case of mismatch, respectively. η is the wave impedance, r the distance from the origin to the field point, and θ the angle between the half-line r and the z-axis. According to the transmission line theory, the current on the long wire antenna can be expressed as

$$I_{CM}(z') = I^+ e^{-\mathrm{j}\beta z'} \left(1 + \Gamma_I e^{-\mathrm{j}2\beta z'} \right) \tag{16}$$

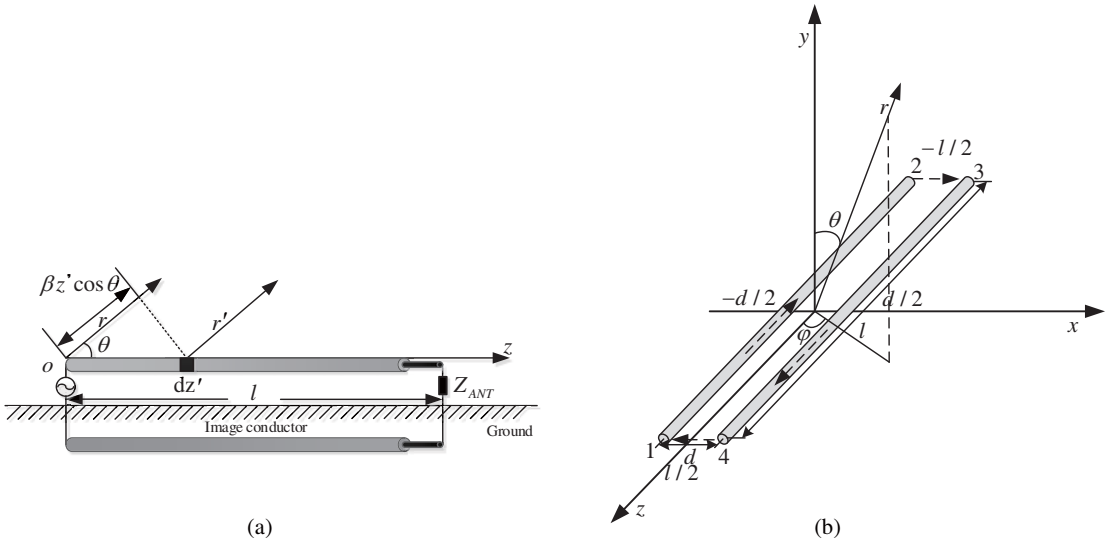

Figure 3. (a) Long wire antenna model. (b) Loop antenna model.

Therefore, in the case of terminal mismatch, the common mode radiation resistance r^{CM} per unit length is

$$r^{CM} = \frac{\eta}{2\pi l}\left[\ln(2\beta l) - 0.4229 + \int_{2\beta l}^{\infty}\frac{\cos\tau}{\tau}\mathrm{d}\tau + \frac{\sin(2\beta l)}{2\beta l}\right]\frac{1+|\Gamma_I|^2}{\left|1+\Gamma_I e^{-\mathrm{j}2\beta l}\right|^2} \tag{17}$$

In addition, considering the line spacing, the parallel two-wire power line is similar to a rectangular shape, so the differential mode radiation model between the two channels of the parallel three-wire power line MIMO-PLC is regarded as the loading ring antenna model of the terminal access resistance, as shown in Fig. 3(b). The distance between the centers of two-wire power lines with length l is d, and φ is the direction angle. Similarly, we can get the current $I_{DM}(z')$ on the loop antenna by referring to Eq. (16).

Similarly, the differential mode radiation resistance r^{DM} per unit length is

$$r^{DM} = \frac{\eta(\beta d)^2}{2\pi l}\left(1 - \mathrm{sinc}(2\beta l)\right)\frac{1+|\Gamma_I|^2}{\left|1+\Gamma_I e^{-\mathrm{j}2\beta l}\right|^2} \tag{18}$$

3. THREE-WIRE POWER LINE CHANNEL MODELING WITH RADIATION LOSS

The equivalent circuit of unit length parameter is introduced into the radiation loss, and the equivalent circuit of unit length parameter including the equivalent radiation resistance of unit length (differential mode and common mode) is given, as shown in Fig. 4.

The unit length resistances r_1' and r_2' of conductor 1 (P neutral line) and conductor 2 (N phase line) containing differential mode radiation loss, and the unit length resistances r_0' of reference 0 conductor (PE protective ground wire) containing common mode radiation loss are as follows

$$\begin{aligned} r_1' &= {r_1}^{DM} + {r_1}^{Ohm} \\ r_2' &= {r_2}^{DM} + {r_2}^{Ohm} \\ r_0' &= r^{CM} + r_0^{Ohm} \end{aligned} \tag{19}$$

Then the corrected unit length resistance matrix R' is

$$R' = \begin{bmatrix} r_1' + r_0' & r_0' \\ r_0' & r_2' + r_0' \end{bmatrix} \tag{20}$$

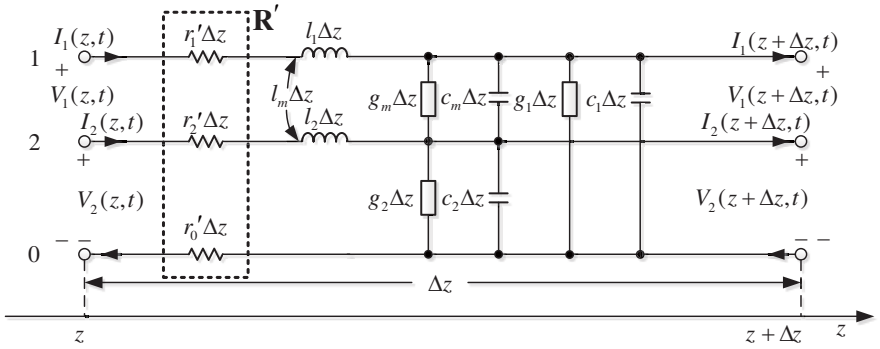

Figure 4. Unit length equivalent circuit including unit length radiation loss.

In this paper, the voltage ratio algorithm proposed in reference [19] is extended to MTL to calculate the transfer function. Referring to Fig. 2, $V(x)$ is the voltage at x, and the corrected voltage ratio of each power line is

$$H_x = \frac{V(x-1)}{V(x)} = \left[I_2 + \Gamma_V'(x-1)\right] T_V' e^{-\gamma' l_x} T_V^{-1\prime} \left[I_2 + \Gamma_V'(x)\right]^{-1} \tag{21}$$

The transfer function of $N+1$ section power line is

$$H(f) = \frac{V(0)}{V(N+1)} = \prod_{x=1}^{N+1} H_x(f) \tag{22}$$

The MIMO-PLC channel model including voltage source and terminal admittance is shown in Fig. 5, where V_g is the voltage source; Z_g is internal admittance; V_1^{Tx} and V_2^{Tx} are transmitter voltage; I_1^{Tx} and I_2^{Tx} are transmitter current; Y_2^{Tx} is the transmitter equivalent admittance; V_1^{Rx} and V_2^{Rx} are receiver voltage; I_1^{Rx} and I_2^{Rx} are receiver current; Y_1^{Rx} and Y_2^{Rx} are receiver equivalent admittance.

Figure 5. MIMO-PLC network with source and terminal.

The equivalent admittance matrix from the $N+1$ node is

$$Y_{eqN+1} = Y_{inN+1} = \begin{bmatrix} Y_{inN+1_{11}} & Y_{inN+1_{12}} \\ Y_{inN+1_{21}} & Y_{inN+1_{22}} \end{bmatrix} \tag{23}$$

$$\begin{bmatrix} I_1^{Tx} \\ I_2^{Tx} \end{bmatrix} = Y_{inN+1} \begin{bmatrix} V_1^{Tx} \\ V_2^{Tx} \end{bmatrix}$$

$$I_2^{Tx} = -Y_2^{Tx} V_2^{Tx} \tag{24}$$

At the sending side,

$$\begin{bmatrix} V_g \\ 0 \end{bmatrix} = \begin{bmatrix} V_1^{Tx} \\ V_2^{Tx} \end{bmatrix} + \begin{bmatrix} Z_g & 0 \\ 0 & 1/Y_2^{Tx} \end{bmatrix} \begin{bmatrix} I_1^{Tx} \\ I_2^{Tx} \end{bmatrix} \tag{25}$$

Consider the internal resistance loss and boundary condition of the sender, where $\alpha_1(f)$ and $\alpha_2(f)$ are the boundary conditions of conductor 1 and conductor 2 of three-wire power line respectively. The result is

$$\begin{aligned}
\alpha_1(f) &= \left[\begin{array}{cc} 1 & -\dfrac{Y_{inN+1_{21}}}{Y_{inN+1_{22}}+Y_2^{Tx}} \end{array}\right]^T \\
\alpha_2(f) &= \left[\begin{array}{cc} -\dfrac{Y_{inN+1_{12}}}{Y_{inN+1_{11}}+Y_1^{Tx}} & 1 \end{array}\right]^T
\end{aligned} \tag{26}$$

$$\begin{aligned}
V_1^{Tx} &= \left(1+Z_gY_{inN+1_{11}}-\frac{Z_gY_{inN+1_{12}}Y_{inN+1_{21}}}{Y_{inN+1_{22}}+Y_2^{Tx}}\right)V_g \\
V_2^{Tx} &= \left(1+Z_gY_{inN+1_{22}}-\frac{Z_gY_{inN+1_{21}}Y_{inN+1_{12}}}{Y_{inN+1_{11}}+Y_1^{Tx}}\right)V_g
\end{aligned} \tag{27}$$

Finally, the SISO-PLC channel transfer function of conductor 1 and conductor 2 is obtained by introducing the radiation loss of differential mode and common mode.

$$\begin{aligned}
H_{SIMO}^1(f) &= 2H(f)\,\alpha_1(f)\,\frac{V_1^{Tx}}{V_g} \\
H_{SIMO}^2(f) &= 2H(f)\,\alpha_2(f)\,\frac{V_2^{Tx}}{V_g}
\end{aligned} \tag{28}$$

After considering the internal resistance loss and boundary conditions of the sender, the radiation model of MIMO-PLC channel transfer function of the final three-wire power line network is $H_{MIMO}(f)$

$$H_{MIMO}(f) = = \left[\begin{array}{cc} H_{SIMO}^1(f) & H_{SIMO}^2(f) \end{array}\right] \tag{29}$$

4. COMPARISON OF SIMULATED AND MEASURED RESULTS

In this paper, the symmetrical structure of $3\times1.5\,\text{mm}^2$ RVV (PVC insulated PVC) national standard copper core power line is used as the test object. The basic parameters of three-wire power line are shown in Table 1, and three-wire power line network parameters are shown in Table 2. The test network is shown in Fig. 6. Vector network analyzer (VNA model E5061B) is used to measure the scattering parameter S_{21} in the 1–200 MHz frequency band of the test network and characterize the MIMO-PLC channel transfer function as shown in Fig. 7. Two MIMO-PLC couplers are connected at both ends of the vector network analyzer and connected with a three-wire power line test network. The test connection modes of common channel and mutual channel are given respectively.

Table 1. Basic parameters of symmetrical three-wire power line.

No.	Parameter	Value
Power line radius	r_w	0.69 mm
Distance between power lines	d	2.5 mm
Conductivity of power line	σ_1	5.8×10^7 S/m
Dielectric leakage conductivity between power lines	σ_2	10^{-5} S/m
Permeability of dielectric between power lines	μ	$4\pi\times10^{-7}$ H/m
Equivalent permittivity of dielectric between power lines	ε	$(3.2/36\pi)\times10^{-9}$ F/m

Equation (29) is used to simulate the test cases shown in Table 2 in the following three situations: differential mode (DM) model, common mode (CM) model, differential and common mode (DM and CM) model. Fig. 8(c) and Fig. 9(c) show that the simulated results are consistent with Fig. 8(b) and

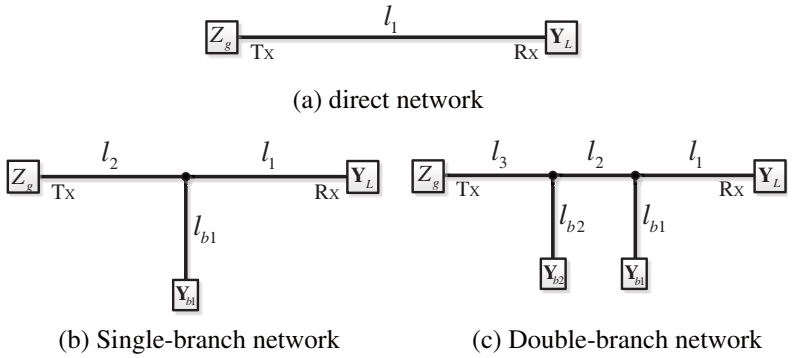

Figure 6. Test network diagram.

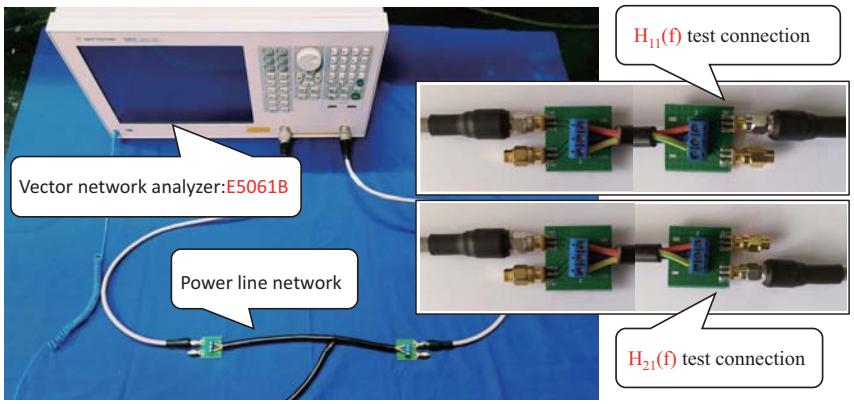

Figure 7. Three-wire power line network test scenario.

Table 2. Three-wire power line network parameters.

Example	$l_{1(m)}$	$l_{2(m)}$	$l_{3(m)}$	$l_{b1(m)}$	$l_{b2(m)}$	Y_{b1}	Y_{b2}
direct network	5	0	0	0	0	0	0
Single-branch network	2	3	0	1	0	open	0
Double-branch network	3	3	4	1	3.8	open	open

Fig. 9(b), respectively. Therefore, for the three-wire power line direct network, the common mode radiation mainly affects the common channel transfer function.

The simulated and measured results of the common channel transfer function $H_{11}(f)$ and mutual channel transfer function $H_{21}(f)$ ($H_{21}(f)$ can be equivalent to crosstalk between unshielded channels) of the single-branch network (the branch terminal is in the open state) are shown in Fig. 10 and Fig. 11. In these three cases, the positions of all grooves (troughs) are consistent. When the common mode radiation factor is added, the results also have a high degree of agreement, which has the same conclusion as direct network.

$H_{11}(f)$ and $H_{21}(f)$ of the double-branch network (branch terminals are all in open state) are shown in Fig. 12 and Fig. 13. The comparison between the basic simulated and measured results shows that there are more grooves in the basic simulated results, but the simulated results obtained by adding the common mode radiation loss factor are consistent with the grooves in the measured results, and the curve shapes are more similar.

By comparing the simulated results with the measured ones in the frequency band of 1–200 MHz

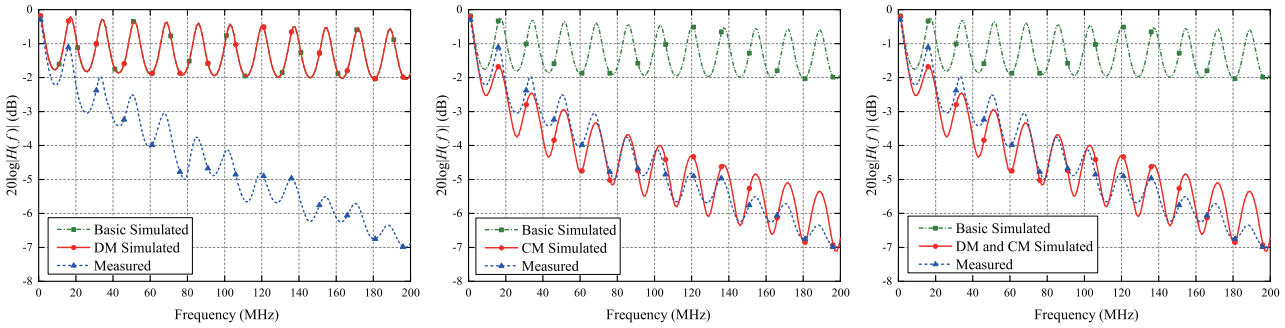

Figure 8. Common channel with radiation loss-$H_{11}(f)$ (direct network). (a) DM simulated and mearured results. (b) CM simulated and mearured results. (c) DM and CM simulated and mearured results.

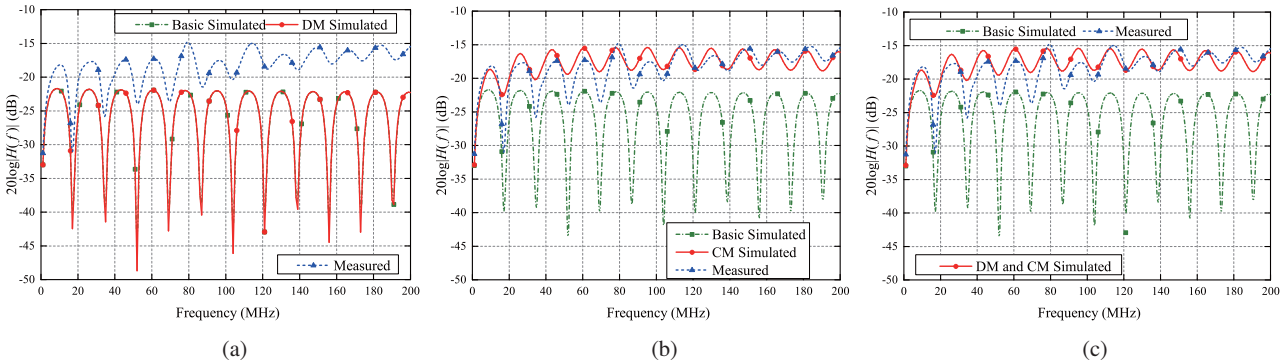

Figure 9. Mutual channel with radiation loss-$H_{21}(f)$ (direct network). (a) DM simulated and mearured results. (b) CM simulated and mearured results. (c) DM and CM simulated and mearured results.

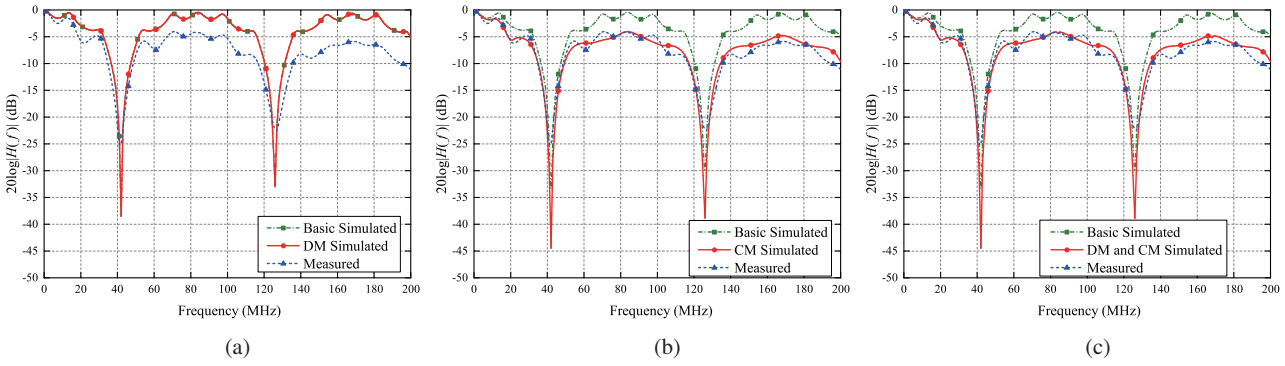

Figure 10. Common channel with radiation loss-$H_{11}(f)$ (Single-branch network). (a) DM simulated and mearured results. (b) CM simulated and mearured results. (c) DM and CM simulated and mearured results.

in Fig. 8–13, it can be concluded that in either case, when differential mode radiation factor is added, it hardly affects the transmission characteristics of the channel transfer function, almost consistent with the simulated results of the basic model; when common mode radiation factor is added, the simulated results of the radiation model are in good agreement with the measured ones (groove position and amplitude size). It is shown that the influence of common mode radiation is greater than that of differential mode radiation.

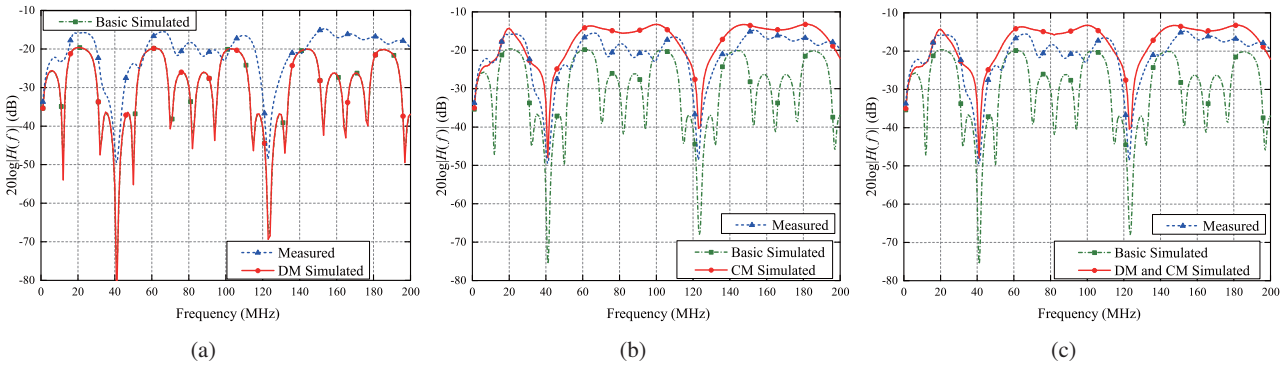

Figure 11. Mutual channel with radiation loss-$H_{21}(f)$ (Single-branch network). (a) DM simulated and mearured results. (b) CM simulated and mearured results. (c) DM and CM simulated and mearured results.

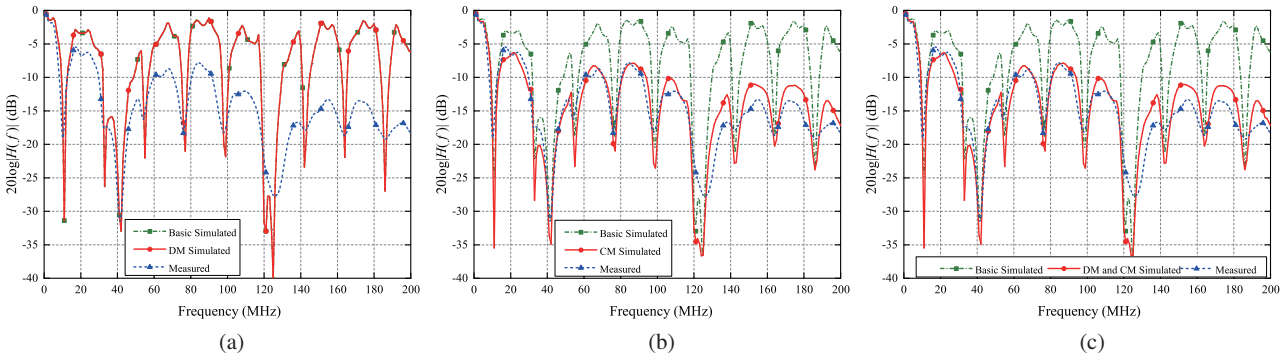

Figure 12. Common channel with radiation loss-$H_{11}(f)$ (Double-branch network). (a) DM simulated and mearured results. (b) CM simulated and mearured results. (c) DM and CM simulated and mearured results.

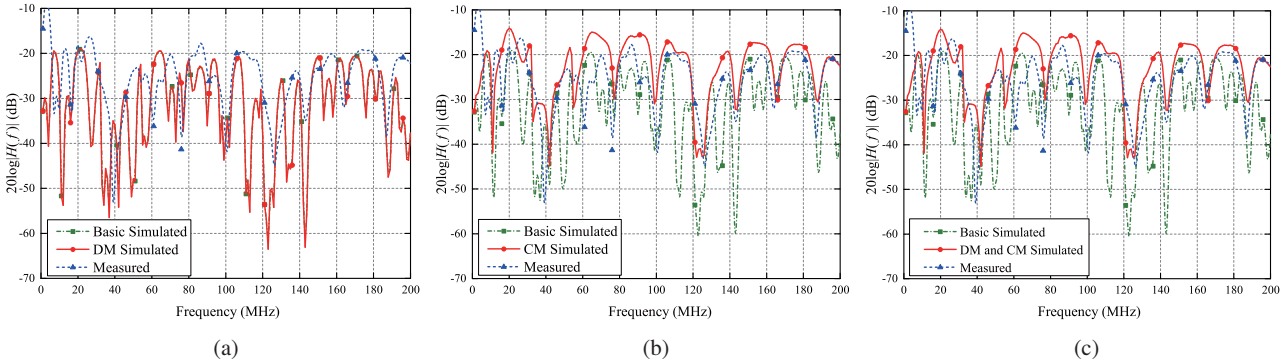

Figure 13. Mutual channel with radiation loss-$H_{21}(f)$ (Double-branch network). (a) DM simulated and mearured results. (b) CM simulated and mearured results. (c) DM and CM simulated and mearured results.

Therefore, the introduction of common mode radiation loss factor into the basic model of MIMO-PLC channel transfer function is beneficial for correcting the difference between channel transfer function and measurement results of the power line network, and the consistency between the simulated results of the radiation model and the measured results verifies the correctness and effectiveness of the modeling.

5. CONCLUSION

In this paper, a PLC channel transfer function model is proposed. In this model, the common and differential mode radiation loss of long wire antenna and the reflection factor in the mismatched transmission line are introduced, and the transfer function is obtained by calculating the voltage ratio between the sender and the receiver. Finally, the numerical simulation and measurement results of MIMO-PLC channel transfer function including radiation loss are compared in three different states. It is verified that the influence of differential mode radiation can be ignored in 1–200 MHz frequency band, and the main factor affecting the transmission characteristics of channel transfer function is common mode radiation. The simulated results of the radiation model are in good agreement with the measured ones, which verifies the accuracy and validity of the MIMO-PLC channel transfer function of three-wire power line including the radiation loss factor. This model lays a foundation for further research on the frequency band pre-selection, power setting, dynamic range design, and MIMO-PLC channel transmission characteristics of power line network channels in complex scenarios.

ACKNOWLEDGMENT

This work was supported by the National Key Research and Development Program of China (Grant No. 2017YFB0308600) and Civil Aviation Joint Fund of the National Natural Science Foundation of China (Grant No. U1733109).

REFERENCES

1. Nassar, M., J. Lin, Y. Mortazavi, A. Dabak, I. H. Kim, and B. L. Evans, "Local utility power line communications in the 3–500 kHz band: Channel impairments, noise, and standards," *IEEE Signal Processing Magazine*, Vol. 29, No. 5, 116–127, 2012.
2. Han, J., C. Choi, W. K. Park, I. Lee, S. H. Kim, and Q. Wu, "PLC-based photovoltaic system management for smart home energy management system," *IEEE Transactions on Consumer Electronics*, Vol. 60, No. 2, 184–189, 2014.
3. Artale, G., A. Cataliotti, V. Cosentino, D. D. Cara, and T. Giovanni, "A new low cost power line communication solution for smart grid monitoring and management," *IEEE Trans. Instrum*, Vol. 21, No. 2, 29–33, 2018.
4. Hashmat, R., P. Pagani, A. Zeddam, and T. Chonavel, "MIMO communications for inhome PLC networks: Measurements and results up to 100 MHz," *IEEE International Symposium on Power Line Communications & Its Applications*, 2010, doi: 10.1109/ISPLC.2010.5479897.
5. Zhang, S., K. Zhao, B. Zhu, Z. Ying, and S. He, "MIMO reference antennas with controllable correlations and total efficiencies," *Progress In Electromagnetics Research*, Vol. 145, 115–121, 2014.
6. Yu, X., L. Wang, H.-G. Wang, X. Wu, and Y.-H. Shang, "A novel multiport matching method for maximum capacity of an indoor MIMO system," *Progress In Electromagnetics Research*, Vol. 130, 67–84, 2012.
7. Khalil, K., M. G. Gazalet, P. Corlay, F. X. Coudoux, and M. Gharbi, "An MIMO random channel generator for indoor power-line communication," *IEEE Transactions on Power Delivery*, Vol. 29, No. 4, 1561–1568, 2014.
8. Shin, J., J. Lee, and J. Jeong, "Channel modeling for indoor broadband power-line communications networks with arbitrary topologies by taking adjacent nodes into account," *IEEE Transactions on Power Delivery*, Vol. 26, No. 3, 1432–1439, 2011.
9. Duche, D. N. and V. Gogate, "Power line communication performance channel characteristics," *Computer Engineering and Applications*, Vol. 3, No. 1, 33–42, 2014.
10. Leone, M. and A. Mantzke, "A foster-type field-to-transmission line coupling model for broadband simulation," *IEEE Transactions on Electromagnetic Compatibility*, Vol. 56, No. 6, 1630–1637, 2014.
11. Versolatto, F. and A. M. Tonello, "An MTL theory approach for the simulation of MIMO power-line communication channels," *IEEE Transactions on Power Delivery*, Vol. 26, No. 3, 1710–1717, 2011.

12. Corchado, J. A., J. A. Cortes, F. J. Canete, and L. Diez, "An MTL-based channel model for indoor broadband MIMO power line communications," *IEEE Journal on Selected Areas in Communications*, Vol. 34, No. 7, 2045–2055, 2016.
13. Pang, T. S., P. L. So, K. Y. See, and A. Kamarul, "Modeling and analysis of common-mode current propagation in broadband power-line communication networks," *IEEE Transactions on Power Delivery*, Vol. 23, No. 1, 171–179, 2008.
14. Righini, D., F. Passerini, and A. M. Tonello, "Modeling transmission and radiation effects when exploiting power line networks for communication," *IEEE Transactions on Electromagnetic Compatibility*, Vol. 60, No. 1, 59–67, 2017.
15. Nasar, S. A. and C. R. Paul, *Essential Engineering Equations*, CRC Press, Boston, 1991.
16. Paul, C. R., "On uniform multimode transmission lines," *IEEE Transactions on Microwave Theory and Techniques*, Vol. 21, No. 8, 556–558, 1973.
17. Paul, C. R., *Modeling of Broadband Power Line Communication Channel Based on Transmission Line Theory and Radiation Loss*, Wiley, New York, 2008.
18. He, D.-L., Y.-Z. Wei, S. Cui, W. Hua, X.-Y Duan, and L. Liu, "Modeling of broadband power line communication channel basedon transmission," *IEICE Electronics Express*, Vol. 16, No. 16, 1–5, 2019.
19. Hasirci, Z. and I. H. Cavdar, "S-parameters-based causal RLGC(f) model of busbar distribution systems for broadband power line communication," *International Journal of Electrical Power & Energy Systems*, Vol. 95, 561–567, 2018.